Analytical and Bioanalytical Chemistry
https://doi.org/10.1007/s00216-020-02448-4

RESEARCH PAPER

Amperometric biogenic amine biosensors based on Prussian blue, indium tin oxide nanoparticles and diamine oxidase– or monoamine oxidase–modified electrodes

Ceren Kaçar[1] · Pınar Esra Erden[2] · Berna Dalkiran[1] · Emine Kübra İnal[1] · Esma Kiliç[1]

Received: 8 November 2019 / Revised: 18 January 2020 / Accepted: 22 January 2020

Abstract

Biogenic amine biosensors, based on screen-printed carbon electrodes (SPCE) modified with Prussian blue (PB) and indium tin oxide nanoparticles (ITONP), are reported. PB/ITONP-modified SPCE was further modified with diamine oxidase (DAO) or monoamine oxidase (MAO) enzymes to construct the biosensors. The morphology of the modified electrodes was studied by scanning electron microscopy (SEM), energy-dispersive X-ray spectroscopy (EDX) and atomic force microscopy (AFM). Cyclic voltammetry (CV) and electrochemical impedance spectroscopy (EIS) were used to enlighten the electrochemical properties of the modified electrodes at each step of biosensor fabrication. Electrode surface composition and experimental conditions were optimized and analytical performance characteristics of the biosensors were studied. Several biogenic amines were tested and both biosensors responded to histamine, putrescine and cadaverine. DAO/ITONP/PB/SPCE biosensor exhibited the highest response to histamine 6.0×10^{-6}–6.9×10^{-4} M with a sensitivity of 1.84 μA mM^{-1}. On the other hand, the highest sensitivity was obtained for cadaverine with the MAO/ITONP/PB/SPCE biosensor. The analytical utility of the presented biosensors were illustrated by the determination of cadaverine and histamine in cheese sample.

Keywords Amperometry · Biosensor · Biogenic amine · Indium tin oxide · Prussian blue · Screen-printed electrode

Introduction

Biogenic amines (BAs), low-molecular-weight organic bases, are formed primarily by the decarboxylation of their precursor amino acids [1]. Histamine, putrescine, cadaverine, tyramine, spermine, β-phenylethylamine, tryptamine and spermidine are found to be the most common BAs present in food products including wine, fish, beer, meat products, seafood, cheese and other dairy products [2]. High levels of certain BAs can be observed in food products as a consequence of microbial contamination and inconvenient conditions during processing and storage [3]. Therefore, the amount of BAs can be used as an indicator for the evaluation of food quality [4]. The ingestion of foods with high biogenic amine content can lead to a health hazard [5]. Hence, the development of rapid, practical, accurate and low-cost methods for BA determination is of great importance in clinical diagnosis and food industry.

Various chromatographic techniques including thin-layer chromatography [6, 7], gas chromatography [8] and high-performance liquid chromatography [9–11] in combination with different detectors were reported for the determination of BAs. However, these techniques usually suffer from tedious sample pretreatments, sophisticated and expensive equipment, long analysis times and require a trained analyst. The use of electrochemical biosensors which offer a sensitive, selective, rapid and low-cost analysis is a promising approach for the determination of BAs [12–16].

In recent years, metal oxide nanoparticle–modified electrodes have found widespread application in (bio)sensors due to their large surface-to-volume ratio, chemical stability and catalytic efficiency [17]. Indium tin oxide (ITO) is probably the most widely used transparent conducting oxide in optoelectronics due to its high electric conductivity and good optic transparency [18]. It

✉ Esma Kiliç
ekilic@science.ankara.edu.tr

[1] Department of Chemistry, Faculty of Science, Ankara University, 06100 Ankara, Turkey

[2] Department of Chemistry, Polatlı Faculty of Science and Arts, Ankara Hacı Bayram Veli University, 06900 Ankara, Turkey

Published online: 19 February 2020

also shows other unique properties such as wide electrochemical working window, low capacitive current, stability, low cost and substrate adhesion which makes it a promising material in biosensor applications [19, 20]. Recently, the use of ITO electrodes in biosensor applications has attracted increasing attention due to its excellent properties and numerous studies have been reported on the fabrication of electrochemical (bio)sensors based on ITO electrodes [20–23]. However, the use of ITO nanoparticles in (bio)sensor development is limited. For example, Sivasakthi et al. prepared nickel-ITO nanocomposite on mild steel substrate via pulse electrodeposition technique and investigated its behaviour as an electrocatalyst for the non-enzymatic sensing of glucose [19]. Rigoni et al. developed ammonia gas sensors using single-walled carbon nanotubes functionalized with ITONP [24]. Bobrowski et al. modified ITO support with ITONP for the development of a self-charging mediator and membrane-less biofuel cell/biosupercapacitor and used it for glucose determination [25].

H_2O_2 is the by-product of the reaction catalysed by a great number of oxidase enzymes [26]. Determination of H_2O_2 is of paramount importance for the oxidase enzyme based biosensors since its concentration is directly proportional to the concentration of the enzymatic substrate. Direct amperometric determination of H_2O_2 at the ordinary electrodes is possible at high potentials. However, at these potentials the presence of easily oxidisable species such as ascorbic acid and uric acid can interfere in the measurement [27]. To overcome this problem, determination of H_2O_2 at low potentials was proposed [28, 29]. Prussian blue (PB), known as artificial enzyme peroxidase, efficiently catalyses the reduction of H_2O_2 at low potentials, offering a sensitive and interference-free detection [30]. Its low cost, selectivity to H_2O_2 reduction in the presence of oxygen and inorganic nature makes PB more suitable than peroxidase enzyme in the fabrication of biosensors [31, 32]. Moreover, the electrodes modified with PB can be used for amperometric determination of other substrates at a low operating potential if combined with H_2O_2 producing oxidase enzymes [31, 33].

Screen-printed electrodes (SPEs) are widely used for the development of single-use biosensors due to their simplicity, low cost, versatility, ease of operation, miniaturization and mass production capabilities [34–37].

The favourable properties of PB and ITONP encouraged us to use these materials for the construction of biogenic amine biosensors. We believe that PB-ITONP composite could be a new sensing platform for biosensor development. Therefore, in the present study, novel biogenic amine biosensors based on ITONP/PB-modified SPCEs were prepared by further immobilizing DAO or MAO enzymes. These biosensors are expected to combine the advantageous properties of ITONP and PB and to exhibit good analytical characteristics.

Experimental

Reagents

DAO (≥ 0.05 unit/mg solid, EC 1.4.3.22 from porcine kidney), MAO A human (≥ 10 unit/mg protein, ≥ 3 mg protein/mL, recombinant, 1 VL, EC 1.4.3.4.), iron (III) chloride, hydrochloric acid, $K_3Fe(CN)_6$, $K_4Fe(CN)_6.3H_2O$, potassium chloride, indium tin oxide nanoparticles (90% In_2O_3 and 10% SnO_2, < 50 nm particle size), sodium monohydrogenphosphate and sodium dihydrogenphosphate, putrescine dihydrochloride, histamine dihydrochloride, cadaverine dihydrochloride, spermine, spermidine, tyramine, tryptamine, 2-phenylethylamine hydrochloride, L-histidine, L-lysine, L-tryptophan, L-phenylalanine, L-tyrosine, L-arginine, gelatin (type A, porcine skin) and Nafion® perfluorinated resin solution, were obtained from Sigma-Aldrich and used as received. L-ornithine hydrochloride was supplied form from Acros Organics. All aqueous solutions were prepared using deionized water. In HPLC studies 1,7-diaminoheptane purchased from Merck and dansyl chloride (1% w/v in acetone) purchased from Fluka were used as the internal standard and derivatization reagent, respectively.

Instrumentation

Electrochemical measurements were carried out on a computer controlled Autolab electrochemical system (Eco-Chemie, Utrecht, The Netherlands) using Nova software (Eco-Chemie). A NT-MDT NTEGRA Solaris instrument was employed for the AFM studies. SEM images were obtained using a Quanta 450 FEG FEI scanning electron microscope. A Bruker detector was utilized to record the EDX spectra. A system consisting of Shimadzu LC-20AT pump, Shimadzu SPD-20A UV-Vis detector (Shimadzu, Japan), Shimadzu CTO-20A oven and an Inertsil ODS-4 (250 × 4.6 mm, 5 μm) column were employed in the HPLC study. The cleanup procedure was conducted using solid-phase extraction (SPE) DSC18 cartridges (Sigma-Aldrich, USA).

Disposable SPCEs (Type C110) consist of a carbon working electrode, a silver pseudo-reference electrode and a carbon auxiliary electrode were obtained from Dropsens. Before modification, electrochemical pretreatment was performed by anodizing the SPCEs at + 1.70 V for 180 s in 50 mM phosphate buffer solution (PBS) (pH 7.4) containing 100 mM KCl [32, 38].

Amperometric experiments were performed in stirred PBS at − 0.15 V.

Preparation of DAO/ITONP/PB/SPCE and MAO/ITONP/PB/SPCE

The biogenic amine biosensors were prepared according to the following procedures:

(1) DAO/ITONP/PB/SPCE: 10 mL of 100 mM $K_3[Fe(CN)]_6$ in 10 mM HCl was mixed with 10 mL of 100 mM $FeCl_3$ in 10 mM HCl to obtain the precursor solution of PB. 20 μL of this precursor solution was dropped onto the working area of SPCE. After 20 min, the SPCE surface was rinsed with a few millilitres of 10 mM HCl and the resulting electrode was left 90 min in the drying-oven at 100 °C to construct the PB/SPCE [32]. Gelatin solution (10 mg mL^{-1}) was prepared by dissolving 100 mg of gelatin in 10 mL deionized water and stirring it until complete dissolution. Gelatin was used as a dispersive agent to obtain stable ITONP dispersions. The ITONP-gelatin dispersion was found to be stable for at least 3 weeks. Twenty milligrams of ITONP were added to 2 mL of gelatin solution, then was ultrasonicated for 1 h to obtain a uniform dispersion. PB/SPCE was modified by a 5 μL of the ITONP mixture (10 mg mL^{-1}) and allowed to dry in air. The enzyme-modified electrode was prepared by casting 10 μL of DAO solution (20 mg mL^{-1}) on the ITONP/PB/SPCE surface and then dried in air. Finally, 3 μL of 0.25% Nafion solution was applied on the resulting electrode in order to minimize the influence of interfering species and this electrode was denoted as DAO/ITONP/PB/SPCE.

(2) MAO/ITONP/PB/SPCE: 5 μL MAO was immobilized onto the ITONP/PB/SPCE using the same procedure explained in section (1) to prepare the MAO/ITONP/PB/SPCE. Construction procedure of the biosensors is shown in Scheme 1.

Real sample analysis

Sample preparation

Cheese samples were purchased from local supermarkets. Twenty grams of cheese were ground and homogenized with 80 mL of 100 mM HCl. The extract was filtered through a Whatman filter paper [39]. The extract mixture was stored at − 18 °C until use.

HPLC analysis

A method slightly modified from the one reported by Zotou et al. was used for the HPLC analysis of the BAs in cheese sample [40]. For this purpose, 1000 mg L^{-1} standard stock solutions of each BA were prepared in water-methanol (1:1) solution and stored at − 18 °C. The corresponding 1000 mg L^{-1} stock solution was diluted with ultrapure water to prepare the solutions at the desired concentrations. A volume of 5 mL of the standard solutions or cheese samples were treated with BR buffer and the pH was adjusted to 9.5. Two hundred microliters of 2424 mg L^{-1} internal standard solution and 800 μL of 1% w/v dansyl chloride solution were added to a 2 mL volume of the resulting reaction solutions and the mixtures were brought to a total volume of 4 mL with acetone-water (3:1 v/v). The final solution was vortexed for 5 min and then kept at 65 °C for 30 min in the dark. DSC-18 cartridge (500 mg 3 mL^{-1}) was activated with 2 mL of methanol and then 2 mL of ultrapure water mixture. After the

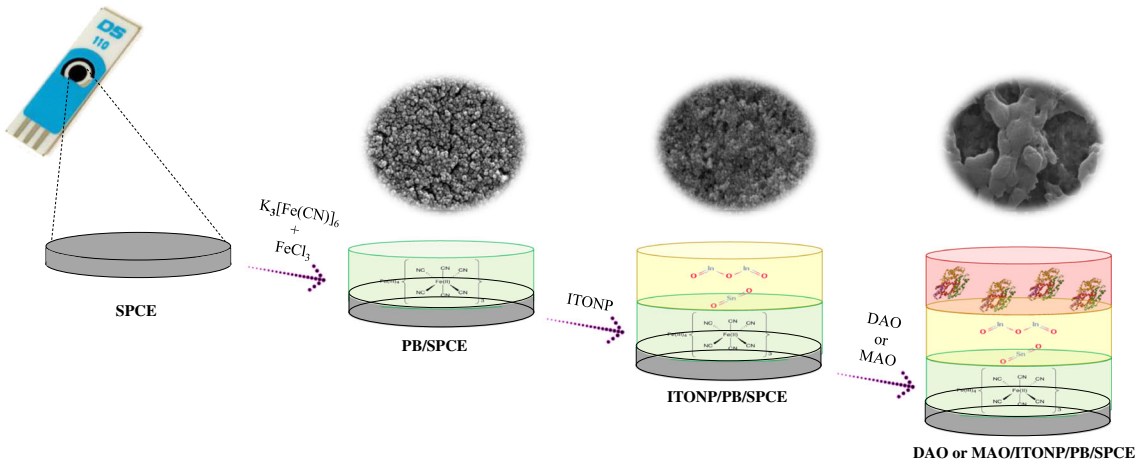

Scheme 1 The construction procedure of the biosensors

dansylated standard solution or the dansylated cheese extract had passed through, the cartridges were washed with 2 mL of acetone-water (1:4 *v*/v) and dried under vacuum. Two milliliters of acetonitrile was used to elute the analytes and the eluate was injected in the HPLC system. The gradient elution program utilized to separate the amines was ultrapure water as solvent A and acetonitrile as solvent B. An initial linear gradient elution from 40% of solvent B to 80% in 25 min was used, followed by another linear elution from 80% to 100% of B in 5 min. The system was equilibrated for 5 min between the analysis. The flow rate was 1 mL min^{-1} and the injection volume was 20 μL. The eluted dansylamides were determined by monitoring their UV absorbance at 254 nm.

Results and discussion

Optimization of the PB formation procedure

The film of PB on the SPCEs was prepared using $K_3[Fe(CN)]_6$ and $FeCl_3$ solutions. Two parameters were optimized for PB formation: (i) formation time of PB on SPCE, (ii) baking time of PB/SPCE in the drying-oven at 100 °C. The optimization study was carried out by changing one parameter at a time and keeping other parameters fixed. Amperometric measurements were recorded at − 0.15 V in PBS (50 mM, pH 8.0) using cadaverine as the reference amine. Firstly, the effect of time on the formation of PB was explored. For this purpose, 20 μL of $FeCl_3$ and $K_3[Fe(CN)_6]$ precursor solution was dropped onto the working area of three bare SPCEs and the electrodes were kept at room temperature for different times of 10, 20 and 30 min. These PB/SPCE-modified electrodes were left at 100 °C in the drying oven for 90 min and then used in the fabrication of DAO/ITONP/PB/SPCE biosensors. The amperometric response of the biosensor to cadaverine was recorded in order to optimize the PB formation time on SPCE (Fig. 1A). The highest cadaverine sensitivity was recorded at the DAO/ITONP/PB/SPCE biosensor fabricated with the PB/SPCE obtained after 20 min and this period was selected as the optimum PB formation time.

After the formation of PB on SPCE, PB/SPCE was baked at 100 °C since it was mentioned in the literature [32] that one-hour baking at 100 °C could obtain a more stable and active layer of PB. In our study, PB/SPCEs were kept in the drying-oven at 100 °C for different times of 30, 60, 90 and 120 min to optimize the baking time. These PB/SPCEs were used for the fabrication of the DAO/ITONP/PB/SPCE biosensors and the highest cadaverine sensitivity was recorded at the DAO/ITONP/PB/SPCE biosensor fabricated with the PB/SPCE obtained after 90 min of baking and this period was selected as the optimum value for PB/SPCE baking (Fig. 1B).

Optimization of the ITONP and enzyme loading

The amounts of loaded ITONP and enzymes during the preparation of the biosensors were also optimized to achieve the maximum sensitivity for the biosensors. Different ITONP loadings (5, 10, 15 and 20 mg mL^{-1}) were used in DAO/ITONP/PB/SPCE biosensor fabrication. As can be seen from Fig. 1C, the sensitivity of the biosensor increased with the

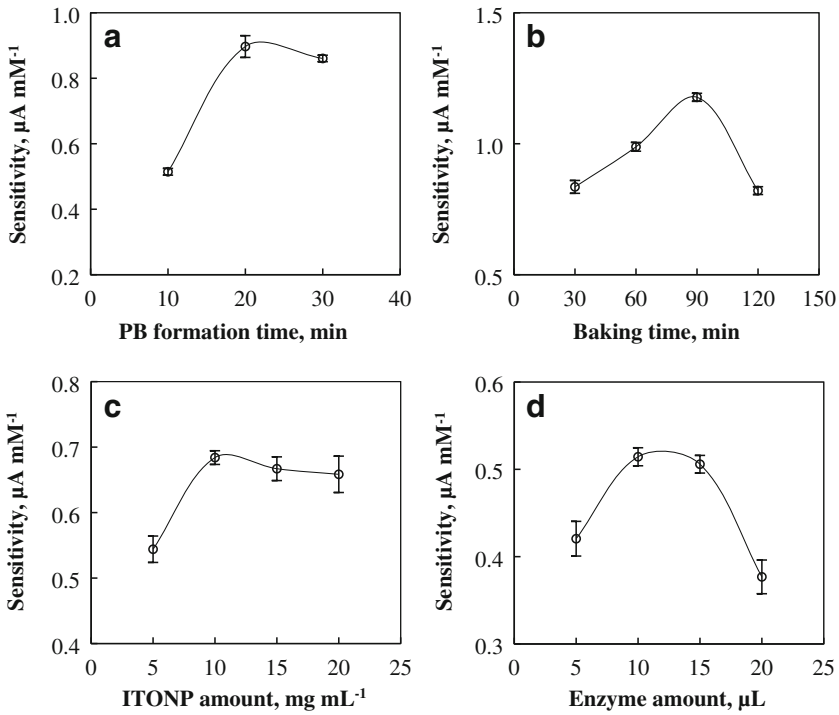

Fig. 1 Effects of (A) PB formation time, (B) baking time, (C) ITONP loading and (D) enzyme loading on the cadaverine response of DAO/ITONP/PB/SPCE (in 0.05 M pH 8.0 PBS, E_{app} = − 0.15 V, Error bars represent the standard deviation for three independent measurements performed with three equally modified electrodes)

ITONP loading up to 10 mg mL^{-1} and then slightly decreased with increasing ITONP loading, which was probably due to an increase in the electron transfer resistance for high nanoparticle loadings [41]. Thus, 10 mg mL^{-1} ITONP was fixed during the present study and this amount was used in the fabrication of DAO/ITONP/PB/SPCE and MAO/ITONP/PB/SPCE biosensors.

In order to investigate the effect of enzyme loading on biosensor response, 5, 10, 15 and 20 μL of DAO solution (20 mg mL^{-1}) was immobilized onto ITONP/PB/SPCEs. Figure 1D shows the sensitivities obtained with different enzyme loadings. The sensitivity of the biosensor improved by increasing the loading of DAO from 5 to 10 μL. Higher enzyme loadings gave a biosensor with a reduced sensitivity. By increasing the DAO loading on the ITONP/PB/SPCE, the enzyme layer on the ITONP/PB matrix becomes denser and could affect the conductor phase within the matrix. This makes the lower response signals at higher enzyme loading [42]. In case of the MAO enzyme, 2.5, 5, 7.5 and 10 μL of enzyme solution was immobilized onto ITONP/PB/SPCEs and four biosensors were fabricated. The sensitivity of the biosensor increased by increasing the MAO loading from 5 to 7.5 μL and decreased afterwards. However, the sensitivities obtained with 5 and 7.5 μL MAO loading were close to each other. Therefore, 5 μL of the enzyme was used in biosensor fabrication.

Surface morphology of modified electrodes

SEM was utilized to investigate the morphology of the electrodes during the modification process. Figure 2A displays the SEM images of (a) SPCE, (b) PB/SPCE, (c) ITONP/SPCE, (d) ITONP/PB/SPCE, (e) DAO/ITONP/PB/SPCE and (f) MAO/ITONP/PB/SPCE. After the modification of SPCE with PB, bright structures of different sizes were observed in the SEM image of PB/SPCE which can be attributed to the formation of PB on SPCE (image b). Image c indicates that the ITO nanoparticles were uniformly dispersed in gelatin without aggregation. The SEM image of ITONP/PB/SPCE (image d) has a highly porous morphology, which provides a larger surface area for enzyme immobilization. Compared with image d, it could be observed that the morphology of DAO/ITONP/PB/SPCE (image e) was obviously changed by immobilization of DAO. On the other hand, a smooth morphology was observed at MAO/ITONP/PB/SPCE (image f) after the modification of the enzyme onto ITONP/PB/SPCE.

EDX measurements were performed to confirm the elemental content of the modified electrodes. EDX spectra and elemental analysis of the (a) PB/SPCE, (b) ITONP/SPCE, (c) ITONP/PB/SPCE and (d) DAO/ITONP/PB/SPCE are depicted in Fig. 2B. The Fe peaks observed at PB/SPCE showed that a PB layer was formed on SPCE. The Fe, In and Sn peaks observed at ITONP/PB/SPCE supported that ITO nanoparticles were modified onto PB/SPCE.

Electrochemical characterization of modified electrodes

The formation of PB on SPCE was verified by cyclic voltammetry measurements. Figure 3A depicts the voltammogram of PB/SPCE recorded between (− 0.50) and (+ 1.1) V at a scan rate of 50 mVs^{-1} in 50 mM PBS (pH 8.0) containing 100 mM KCl. The typical two pairs of redox peaks indicating the oxidation and reduction of PB confirms the formation of PB on SPCE. These redox pairs correspond to the conversion of Prussian white to PB (0.23/− 0.03 V) and PB to Berlin green (0.88/0.72 V). The first redox couple (0.23/− 0.03 V) is related to the oxidation of Prussian white and reduction of PB. The second redox couple (0.88/0.72 V) is related to the oxidation of PB and reduction of Berlin green [32, 43].

The modification steps of the surface-modified electrodes can be monitored by the cyclic voltammetry of $[Fe(CN)_6]^{3-}/[Fe(CN)_6]^{4-}$ redox probe. Figure 3B displays the CV curves of (a) SPCE, (b) PB/SPCE, (c) ITONP/PB/SPCE and (d) DAO/ITONP/PB/SPCE in the solution containing 5.0 mM $[Fe(CN)_6]^{3-}/[Fe(CN)_6]^{4-}$ and 100 mM KCl at 50 mVs^{-1}. At bare SPCE (curve a) the peaks of the redox couple were observed. After the formation of PB on SPCE (curve b) the redox peak currents significantly increased and peak-to-peak separation (ΔEp) decreased. The highest peak current was observed at ITONP/PB/SPCE (curve c) which suggests that electron transfer at ITONP/PB/SPCE is faster than the other electrodes and ITONP/PB matrix can improve the transmission of electrons between the redox probe and the SPCE [44]. After the modification of the ITONP/PB/SPCE surface with DAO, a decrease of peak currents was observed (curve d) indicating that the presence of insulating enzyme layer on the electrode surface hindered the electron transfer. The cyclic voltammograms of the ITONP/PB/SPCE were recorded between (− 0.40) and (+ 0.40) V at different scan rates in 50 mM PBS containing 100 mM KCl. Figure 3C depicts the plot of anodic and cathodic peak currents vs. scan rate. With scan rate increasing from 10 to 100 mVs^{-1}, peak currents increased linearly, indicating a surface controlled behaviour [45].

Figure 3D presents the Nyquist curves of (a) SPCE, (b) PB/SPCE and (c) ITONP/PB/SPCE obtained in the solution containing 5.0 mM $[Fe(CN)_6]^{3-}/[Fe(CN)_6]^{4-}$ and 100 mM KCl. During the EIS measurements the frequency ranged from 10^5 to 0.05 Hz and the amplitude was 10 mV. The measurements were performed under open circuit potential (OCP) conditions. The bare SPCE (data not shown) showed the highest electron transfer resistance (R_{ct}) (3000 Ω). However, the R_{ct} values obtained with PB/SPCE (80 Ω) and ITONP/PB/SPCE (11 Ω) were very small indicating that these electrodes had

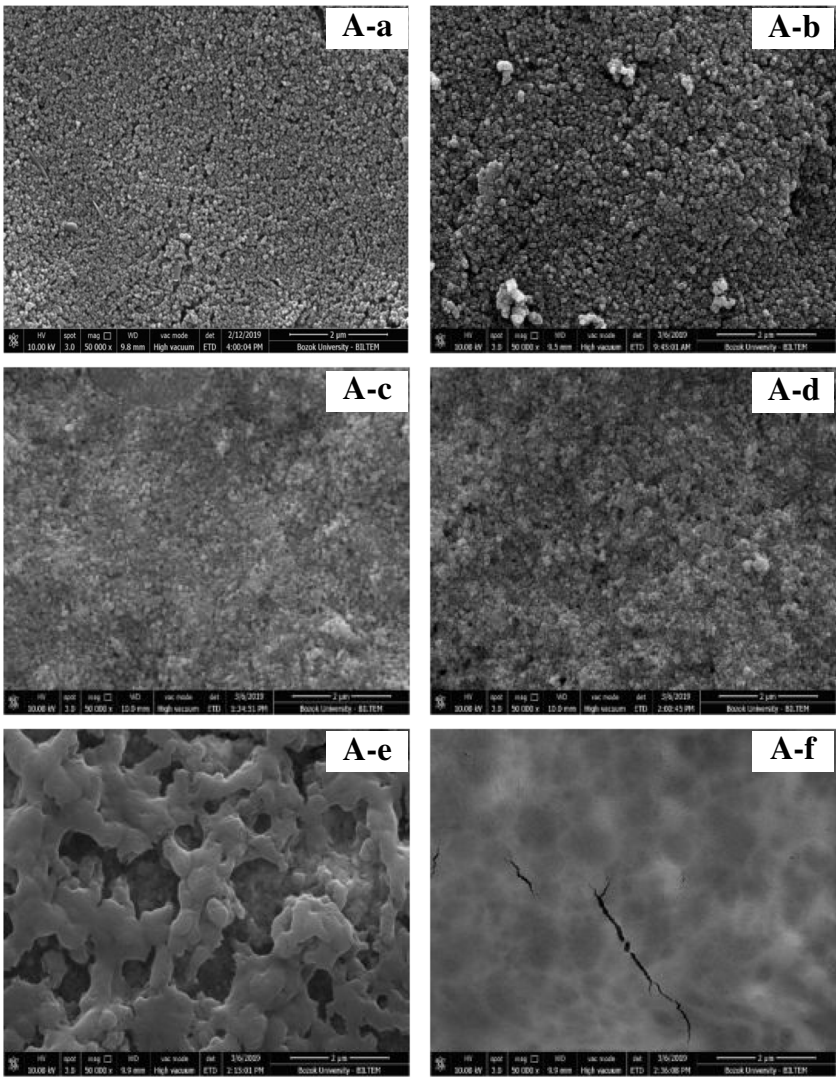

Fig. 2 (A) SEM images of (a) SPCE, (b) PB/SPCE, (c) ITONP/SPCE, (d) ITONP/PB/SPCE, (e) DAO/ITONP/PB/SPCE and (f) MAO/ITONP/PB/SPCE (2 μm; EHT = 10.00 kV; Mag = × 50.000). (B) EDX spectra and elementel analysis (inset) of (a) PB/SPCE, (b) ITONP/SPCE, (c) ITONP/PB/SPCE and (d) DAO/ITONP/PB/SPCE

higher electrical conductivity than the bare SPCE surface and thereby improved electron transfer.

Optimization of experimental parameters

Optimization of working potential is crucial to achieve the best biosensor response. The influence of working potential on the amperometric response of DAO/ITONP/PB/SPCE was investigated in the range from (− 0.20) to (+ 0.05) V in 50 mM pH 8.0 PBS including 0.03 mM cadaverine. The response current of the DAO/ITONP/PB/SPCE decreased as the working potential was changed from − 0.20 V to + 0.05 V. However, the linearity and repeatability of the calibration curves plotted at − 0.20 V were not satisfactory. At − 0.15 V, better results were obtained for these performance parameters. Thus, − 0.15 V was selected as the working potential in subsequent experiments. This potential was also used in the experiments performed with MAO/ITONP/PB/SPCE.

DAO enzyme catalyses the oxidative deamination of various BAs to the corresponding aldehydes and NH_3 with H_2O_2 production (Eq. 1). In our study, H_2O_2 produced by the enzymatic reaction is reduced by the artificial peroxidase PB (Eq. 2). In the literature, it was reported that PBred ($K_4Fe_4[Fe(CN)_6]_3$) on the electrode surface catalyses the reduction of H_2O_2 via a four electron reaction and insoluble PBox ($Fe_4[Fe(CN)_6]_3$) is formed [46, 47]. PBox is then electro-reduced on DAO/ITONP/PB/SPCE surface (Eq. 3). The reduction current measured is directly proportional to the concentration of the corresponding biogenic amine.

$$RCH_2NH_2 + O_2 \overset{DAO}{\rightarrow} RCHO + H_2O_2 + NH_3 \quad (1)$$

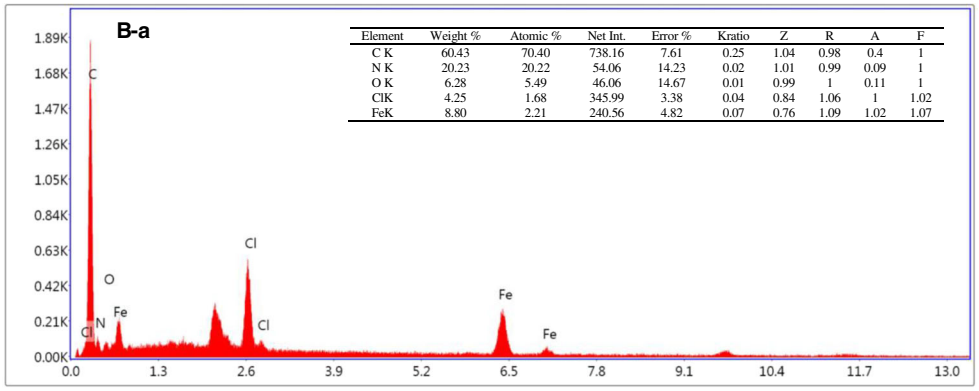

Element	Weight %	Atomic %	Net Int.	Error %	Kratio	Z	R	A	F
C K	60.43	70.40	738.16	7.61	0.25	1.04	0.98	0.4	1
N K	20.23	20.22	54.06	14.23	0.02	1.01	0.99	0.09	1
O K	6.28	5.49	46.06	14.67	0.01	0.99	1	0.11	1
ClK	4.25	1.68	345.99	3.38	0.04	0.84	1.06	1	1.02
FeK	8.80	2.21	240.56	4.82	0.07	0.76	1.09	1.02	1.07

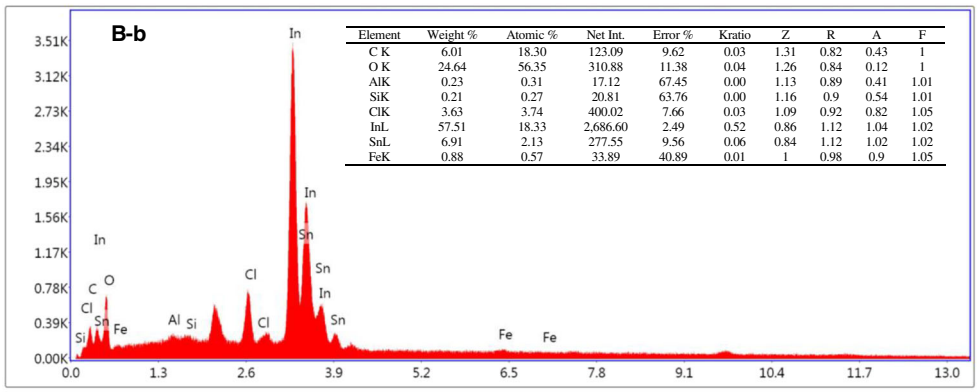

Element	Weight %	Atomic %	Net Int.	Error %	Kratio	Z	R	A	F
C K	6.01	18.30	123.09	9.62	0.03	1.31	0.82	0.43	1
O K	24.64	56.35	310.88	11.38	0.04	1.26	0.84	0.12	1
AlK	0.23	0.31	17.12	67.45	0.00	1.13	0.89	0.41	1.01
SiK	0.21	0.27	20.81	63.76	0.00	1.16	0.9	0.54	1.01
ClK	3.63	3.74	400.02	7.66	0.03	1.09	0.92	0.82	1.05
InL	57.51	18.33	2,686.60	2.49	0.52	0.86	1.12	1.04	1.02
SnL	6.91	2.13	277.55	9.56	0.06	0.84	1.12	1.02	1.02
FeK	0.88	0.57	33.89	40.89	0.01	1	0.98	0.9	1.05

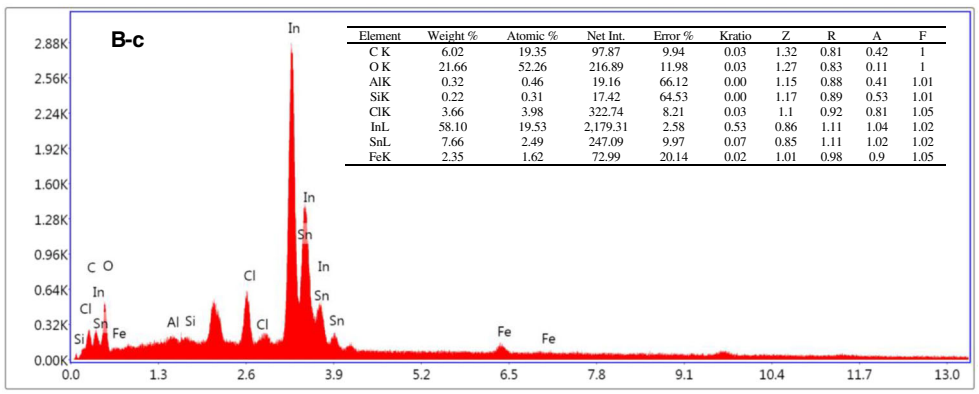

Element	Weight %	Atomic %	Net Int.	Error %	Kratio	Z	R	A	F
C K	6.02	19.35	97.87	9.94	0.03	1.32	0.81	0.42	1
O K	21.66	52.26	216.89	11.98	0.03	1.27	0.83	0.11	1
AlK	0.32	0.46	19.16	66.12	0.00	1.15	0.88	0.41	1.01
SiK	0.22	0.31	17.42	64.53	0.00	1.17	0.89	0.53	1.01
ClK	3.66	3.98	322.74	8.21	0.03	1.1	0.92	0.81	1.05
InL	58.10	19.53	2,179.31	2.58	0.53	0.86	1.11	1.04	1.02
SnL	7.66	2.49	247.09	9.97	0.07	0.85	1.11	1.02	1.02
FeK	2.35	1.62	72.99	20.14	0.02	1.01	0.98	0.9	1.05

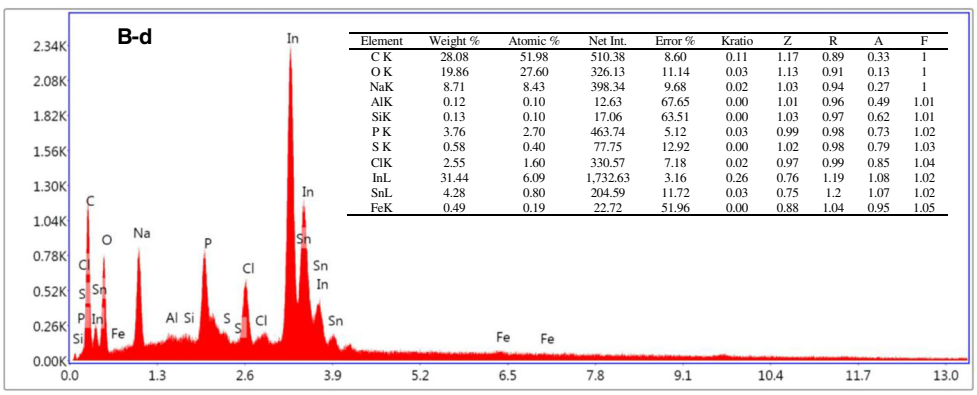

Element	Weight %	Atomic %	Net Int.	Error %	Kratio	Z	R	A	F
C K	28.08	51.98	510.38	8.60	0.11	1.17	0.89	0.33	1
O K	19.86	27.60	326.13	11.14	0.03	1.13	0.91	0.13	1
NaK	8.71	8.43	398.34	9.68	0.02	1.03	0.94	0.27	1
AlK	0.12	0.10	12.63	67.65	0.00	1.01	0.96	0.49	1.01
SiK	0.13	0.10	17.06	63.51	0.00	1.03	0.97	0.62	1.01
P K	3.76	2.70	463.74	5.12	0.03	0.99	0.98	0.73	1.02
S K	0.58	0.40	77.75	12.92	0.00	1.02	0.98	0.79	1.03
ClK	2.55	1.60	330.57	7.18	0.02	0.97	0.99	0.85	1.04
InL	31.44	6.09	1,732.63	3.16	0.26	0.76	1.19	1.08	1.02
SnL	4.28	0.80	204.59	11.72	0.03	0.75	1.2	1.07	1.02
FeK	0.49	0.19	22.72	51.96	0.00	0.88	1.04	0.95	1.05

Fig. 2 continued.

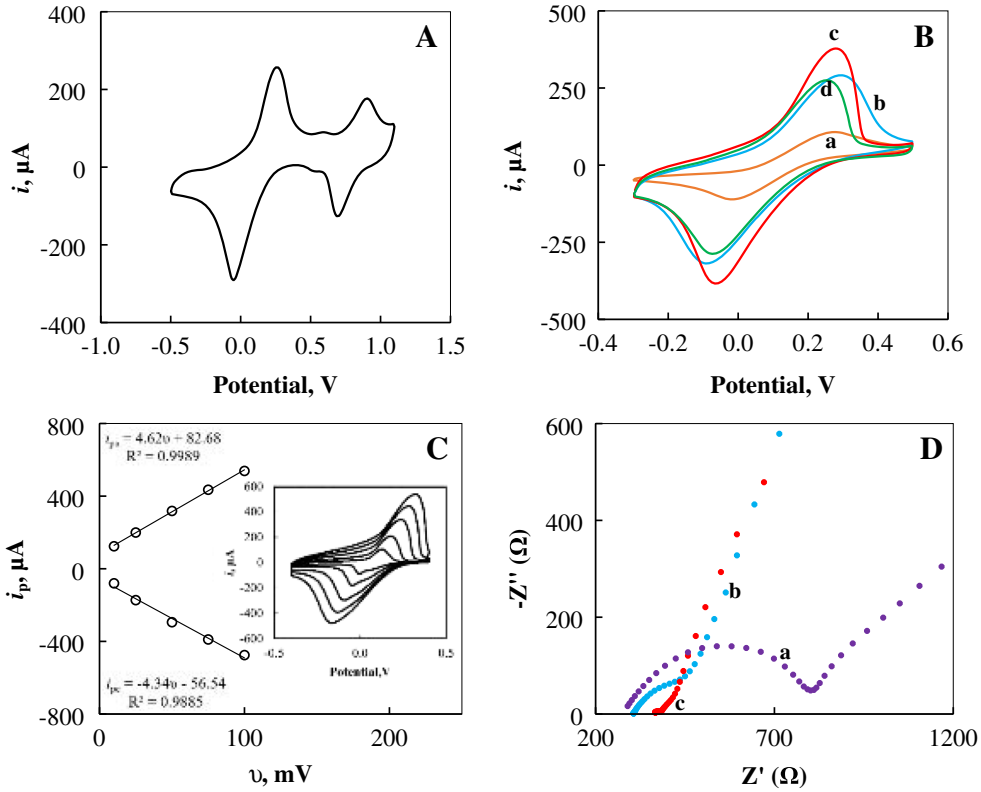

Fig. 3 (A) Cyclic voltammogram of PB/SPCE (50 mM PBS containing 100 mM KCl), (B) Cyclic voltammograms of (a) SPCE, (b) PB/SPCE, (c) ITONP/PB/SPCE and (d) DAO/ITONP/PB/SPCE (5.0 mM $[Fe(CN)_6]^{3-}/[Fe(CN)_6]^{4-}$ solution containing 100 mM KCl), (C) The plots of anodic and cathodic peak currents vs. scan rate (inset: Cyclic voltammograms of ITONP/PB/SPCE at different scan rates in 50 mM PBS containing 100 mM KCl) and (D) Nyquist curves of (a) ITONP/SPCE, (b) PB/SPCE and (c) ITONP/PB/SPCE (5.0 mM $[Fe(CN)_6]^{3-}/[Fe(CN)_6]^{4-}$ solution containing 100 mM KCl)

$$PB_{red} + 2H_2O_2 \rightarrow PB_{ox} + 4K^+ + 4OH^- \quad (2)$$

$$PB_{ox} + 4e^- \leftrightarrow PB_{red} \quad (3)$$

pH of the supporting solution plays a critical role in achieving good analytical performance. Therefore, the effect of pH on the catalytic activity of immobilized DAO and MAO was investigated for three biogenic amines (cadaverine, histamine and putrescine) in 50 mM PBS. The concentration for each biogenic amine tested was 0.03 mM and the current responses of the biosensors were recorded. Figure 4 displays the dependence of DAO/ITONP/PB/SPCE and MAO/ITONP/PB/SPCE response on pH. As can be seen from this figure, with the DAO/ITONP/PB/SPCE biosensor, maximum response current was obtained at pH 7.5, pH 8.0 and pH 8.0 for histamine, putrescine and cadaverine, respectively. In case of MAO/ITONP/PB/SPCE biosensor, optimum pH values were selected as 8.5 for histamine, 7.5 for putrescine and pH 8.0 for cadaverine. These optimum pH values were used for the corresponding biogenic amine determination with both biosensors.

Performance parameters

The chronoamperometric responses at the DAO/ITONP/PB/SPCE and MAO/ITONP/PB/SPCE biosensors for the successive addition of cadaverine with different concentrations were recorded. Figure 5 displays the calibration curves of (A) DAO/ITONP/PB/SPCE and (B) MAO/ITONP/PB/SPCE biosensors. DAO/ITONP/PB/SPCE biosensor exhibited a linear range for cadaverine concentration from 6.0×10^{-6} to 1.0×10^{-3} M ($R^2 = 0.992$) with a detection limit of 2.7×10^{-6} M and sensitivity of 0.65 µA mM^{-1} (Fig. 5A-a). In case of MAO/ITONP/PB/SPCE biosensor the linear working range for cadaverine was 3.0×10^{-6}–1.0×10^{-3} M ($R^2 = 0.990$) with a detection limit of 8.9×10^{-7} M and sensitivity of 0.57 µA mM^{-1} (Fig. 5B-a).

The amperometric responses of putrescine, histamine, tyramine, phenylethylamine, tryptamine, spermine and spermidine at DAO/ITONP/PB/SPCE and MAO/ITONP/PB/SPCE biosensors were also investigated. Both biosensors exhibited good substrate selectivity for histamine and putrescine. The biosensors did not respond to other BAs investigated. The performance parameters obtained for cadaverine, histamine and putrescine with DAO/ITONP/PB/SPCE and MAO/ITONP/PB/SPCE biosensors are presented in Table 1. DAO/ITONP/PB/SPCE showed the best sensitivity (1.84 µA mM^{-1}) for histamine with a linear working range of 6.0×10^{-6}–6.9×10^{-4} M (Fig. 5A-b). The linear ranges obtained for putrescine (7.9×10^{-6}–3.0×10^{-3} M with a sensitivity of 0.44 µA mM^{-1}) (Fig. 5A-c) and cadaverine (6.0×10^{-6}–1.0×10^{-3} M) (Fig. 5A-a) were wider than that of histamine. On the other hand, MAO/ITONP/PB/SPCE exhibited the highest sensitivity to cadaverine (0.57 µA mM^{-1}) with a linear range of 3.0×10^{-6}–1.0×10^{-3} M (Fig. 5B-a). The response

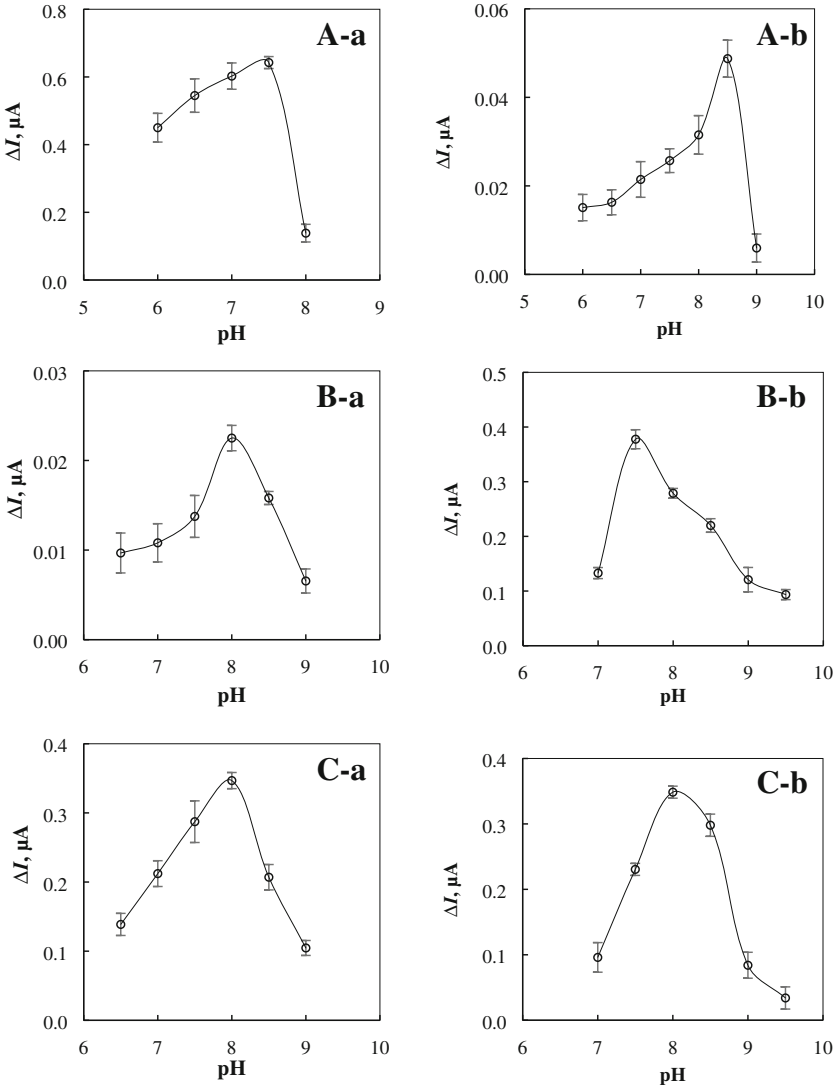

Fig. 4 Effect of pH on the response of (a) DAO/ITONP/PB/SPCE and (b) MAO/ITONP/PB/SPCE: (A) histamine, (B) putrescine and (C) cadaverine (in 0.05 M PBS containing 0.03 mM biogenic amine, $E_{app} = -0.15$ V)

current of this biosensor was proportional to the concentration of putrescine in two linear ranges from 4.0×10^{-6} to 1.2×10^{-4} M with a sensitivity of 0.22 μA mM^{-1} and from 2.9×10^{-4} to 3.9×10^{-3} M with a sensitivity of 0.03 μA mM^{-1} (Fig. 5B-c). MAO/ITONP/PB/SPCE biosensor also displayed a wide linear response to histamine ranging from 2.0×10^{-6} to 3.2×10^{-2} M (Fig. 5B-b). The response times of the DAO/ITONP/PB/SPCE and MAO/ITONP/PB/SPCE biosensors were < 40 s for the BAs studied.

Biosensor repeatability refers to the repetitive measurements performed by using a single biosensor to check variations in its response. Biosensor reproducibility on the other hand refers to

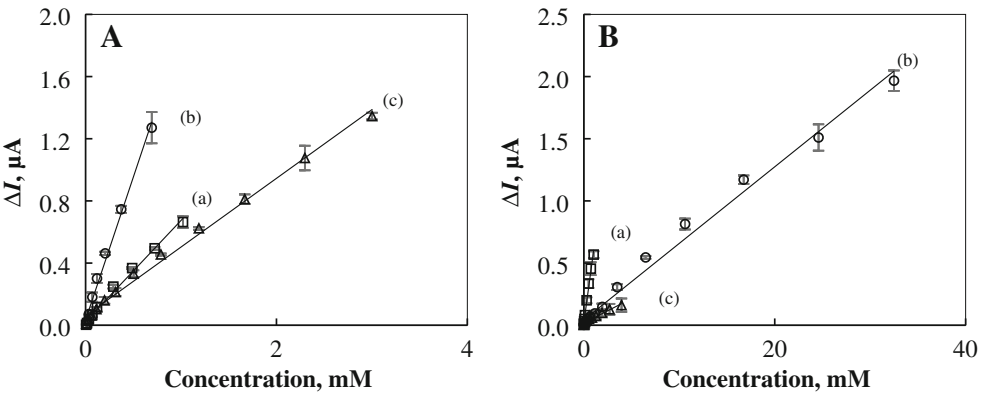

Fig. 5 Calibration graphs of (A) DAO/ITONP/PB/SPCE and (B) MAO/ITONP/PB/SPCE for (a) cadaverine, (b) histamine and (c) putrescine (in 0.05 M PBS, $E_{app} = -0.15$ V)

Table 1 Comparison of the analytical performances of different biogenic amine biosensors

Modified electrode (biosensor)	Substrate	Potential/pH	LOD	Linear working range	Sensitivity	Sample	Ref.
DAO/ITONP/PB/SPCE	His	−0.15 V/7.5	1.9 μM	6–690 μM	1.84 μA mM^{-1}	Cheese	This work
	Put	−0.15 V/8.0	7.8 μM	7.9–3000 μM	0.44 μA mM^{-1}		
	Cad	−0.15 V/8.0	2.7 μM	6–3000 μM	0.65 μA mM^{-1}		
MAO/ITONP/PB/SPCE	His	−0.15 V/8.5	2.0 μM	2–32,000 μM	0.06 μA mM^{-1}	Cheese	This work
	Put	−0.15 V/7.5	3.8 μM	4–120 μM 290–3900 μM	0.22 μA mM^{-1} 0.03 μA mM^{-1}		
	Cad	−0.15 V/8.0	0.9 μM	3–1000 μM	0.57 μA mM^{-1}		
DAO-HRP- PVI7-dme-Os -PEGDGE/Graphite electrode	His	−0.05 V/7.0	5 μM	10–500 μM	–	Pork, fish	[12]
DAO-HEMA film/Carbon paste SPE	His	+0.35 V/7.4	3.5 μM	0–326 μM	1.02 μA mM^{-1}	Tiger prawn	[48]
DAO-HRP/HOMeFc/SPE MAO-HRP/HOMeFc/SPE	His	+0.25 V/9.3	0.2 μM 0.4 μM	0.2–1.6 μM 0.4–2.4 μM	–	Fish	[49]
DAO-HRP/PS-MWCNT-Fc/SPE	His	−0.05 V/8.0	0.2 μM	0.3–20 μM	0.019 μA μM^{-1}	Fish	[50]
DAO/CeO_2–PANI/GCE	His	−0.10 V/7.4	48.8 μM	450–1050 μM	0.725 μA cm^{-2} μM^{-1}	Tiger prawn	[51]
LSG-nCu-CNC/DAO LSC-nCu-MFC/DAO	His	+0.50 V/7.4	7.7 μM 11.6 μM	50–1600 μM	58.7 μA mM^{-1}23.3 μA mM^{-1}	Fish	[52]
DAO/BSA/GA/SPE	His	−0.30 V/7.2	4.5 μM	9–675 μM	0.42 μA mM^{-1}	Fish	[53]
DAO/PB/SPE	Put	−0.05 V/7.4	10 μM	20–300 μM	–	Human saliva	[54]
DAO-PAP/Dual-Au-SPE	Put	+0.70 or +0.60 V/7.4	2.3 μM	7.9–227 μM	0.99 μA mM^{-1}	Wine, beer	[55]
DAO-nano-Fe_3O_4/GCE	Put	+0.40 V/7.2	6.5×10^{-4} μM	0.002–0.008 μM	–	–	[56]
Chitosan/DAO/CeO_2/GCE	Put	+0.73 V/7.4	0.01 μM	0.1–5000 μM	–	Tiger prawn	[57]
MAO/TTF/SPCE	Put	+0.25 V/11.0	17.2 μM	16–101 μM	–	Zucchini, anchovies	[58]
AO-HRP-PVI_{13}-dmeOs-PEGDGE/graphite electrode	His	−0.05 V/7.2	0.3 μM	1–150 μM	0.073 μA μM^{-1} cm^{-2}	Fish	[59]
	Put		0.2 μM	1–400 μM	0.194 μA μM^{-1} cm^{-2}		
DAO-MB-Co(II)-phthalocyanine/CE	His	+0.40 V/7.2	His: 5.1 Put: 1.0 Cad: 0.6 μM	His: 4.5–5.13 μM	His: 0.13 Put:2.11 Cad:3.03 nA μM^{-1}	Fish	[13]
DAO-MB-PB/CE	Put	−0.10 V/7.2	His: 4.8 Put:0.9 Cad:0.7 μM	Put: 0.90–1.03 μM	His: 0.57 Put: 3.22 Cad: 3.12 nA μM^{-1}		
DAO-MB-Os-wired HRP-modified CE	Cad	+0.05 V/7.2	His: 4.5 Put:0.9 Cad:0.5 μM	Cad: 0.47–0.60 μM	His: 0.31 Put: 3.31 Cad: 2.61 nA μM^{-1}		
MAO/AuNPs/TTF/SPCE	Put	+0.25 V/11.0	9.9 μM	9.9–74.1 μM	1.18×10^{-3} μA μM^{-1}	Octopus	[3]
	Cad		19.9 μM	19.6–107.1 μM	1.14×10^{-3} μA μM^{-1}		
DAO/PEDOT/Pt	Put	+0.70 V/8.4	30 μM	30–430 μM	2.13×10^{-4} μA μM^{-1} mm^{-2}	–	[60]

Table 1 (continued)

Modified electrode (biosensor)	Substrate	Potential/pH	LOD	Linear working range	Sensitivity	Sample	Ref.
	Cad		60 μM	60–250 μM	1.39×10^{-4} μA μM^{-1} mm^{-2}		

BSA: bovine serum albumin; *CE*: carbon electrode; *CNC*: nanocrystalline cellulose hydrogel; *Fc*: ferrocene; *GA*: glutaraldehyde; *GCE*: glassy carbon electrode; *HEMA*: 2-hydroxyethyl metacrylate; *HOMeFc*: hydroxymethylferrocene; *HRP*: horseradish peroxidase; *LSG*: laser scribed graphene; *MFC*: microfibrilated cellulose; *MB*: magnetic beads; *PANI*: polyaniline; *PAP*: polyazeti-dine prepolimer; *PB*: Prussian blue; *PEDOT*: poly(3,4-ethylenedioxythiophene); *PEGDGE*: poly(ethylene glycol) (400) diglycidyl ether; *PS*: polysulfone; *PVI13-dmeOs*: poly(1-vinylimidazole)-[Os(4,4′-dimethylbipyridine)$_2$Cl]$^{+/2+}$ complex; *PVI7-dme-Os*: poly(vinylimidazole)-Os(4,4′-dimethylbipyridine)$_2$Cl complex; *TTF*: tetrathiofulvalene

the biosensor variations in response between individual members of a batch of similarly fabricated biosensors. In this study, the repeatability and reproducibility of the biosensors were evaluated using histamine for DAO/ITONP/PB/SPCE and cadaverine for MAO/ITONP/PB/SPCE. Four calibration curves were recorded under the optimum experimental conditions, using the same electrode to evaluate the repeatability and different electrodes in the case of reproducibility. The slopes of these calibration curves were utilized to calculate these parameters in terms of relative standard deviation (RSD), yielding values of 3.4% and 4.3% for the reproducibility and repeatability of DAO/ITONP/PB/SPCE, respectively. The reproducibility and repeatability of the MAO/ITONP/PB/SPCE biosensor were also checked and RSD values were calculated to be 1.5% and 5.8%, respectively. These results indicate that the presented biosensors exhibit good repeatability and reproducibility. The operational stability of the presented biosensors was investigated by successive measurements of the DAO/ITONP/PB/SPCE response to 0.2 mM histamine and MAO/ITONP/PB/SPCE response to 0.2 mM cadaverine. Both biosensors exhibited good operational stability, and no significant decrease (RSD < 10% for DAO/ITONP/PB/SPCE and < 5% for MAO/ITONP/PB/SPCE) was observed after 50 measurements. The good stability obtained for the DAO/ITONP/PB/SPCE and MAO/ITONP/PB/SPCE biosensors indicates the suitability of the PB/ITONPs/gelatin matrix to preserve the activity of the enzymes for long-term operation.

In order to evaluate the performance of the DAO/ITONP/PB/SPCE and MAO/ITONP/PB/SPCE biosensors, analytical characteristics in terms of linear working range, detection limit and sensitivity were compared with previously reported amperometric BA biosensors based on DAO and MAO enzymes as presented in Table 1. Results showed that the DAO/ITONP/PB/SPCE and MAO/ITONP/PB/SPCE biosensors exhibited better performance than most of the other BA biosensors in terms of lower detection limit and wider linear dynamic range.

The possible interference of various amino acids on biosensor response were investigated. The amino acids selected in this study were those involved in the biosynthesis of BAs, namely tyrosine, histidine, lysine, tryptophan, arginine, ornithine and phenylalanine [61]. Histamine and cadaverine were selected as the reference amines for the DAO/ITONP/PB/SPCE and MAO/ITONP/PB/SPCE, respectively. The interference effect was evaluated by comparison of the signal obtained for 0.04 M biogenic amine standard solution vs. the signal obtained for solutions of the same concentration of those amino acids. Figure 6 shows that most of the amino acids have a slightly influence (< 10%) on biosensor response. However, the presence of equal amount of histidine and lysine cause significant interference on the response currents of DAO/ITONP/PB/SPCE (34.0%) and MAO/ITONP/PB/SPCE (22.3%), respectively and their presence in real sample can affect the biosensor response.

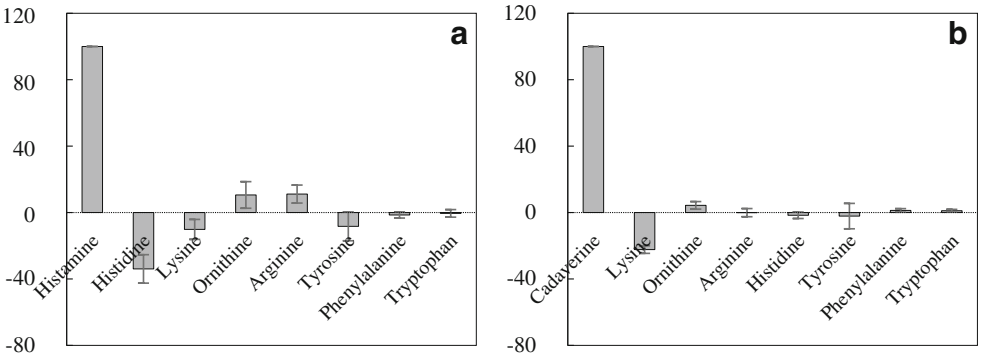

Fig. 6 Effect of various amino acids on the response of (A) DAO/ITONP/PB/SPCE and (B) MAO/ITONP/PB/SPCE biosensors (in 0.05 M PBS, $E_{app} = -0.15$ V)

Real sample analysis

In order to investigate their application in real sample analysis, the biosensors were employed in cheese samples. Turkish white cheese, aged kashar cheese and İzmir tulum cheese were used for the real sample analysis. Among these cheese samples İzmir Tulum cheese was stored at +4 °C in vacuum sealed package and analysed 18 months after its stated expiration date. Conventional HPLC method was used to validate the results obtained using the DAO/ITONP/PB/SPCE and MAO/ITONP/PB/SPCE biosensors. For this purpose, histamine and cadaverine levels in three different types of cheese samples were analysed by the HPLC method and also by the presented biosensors. Each sample was analysed in triplicate.

The results of the chromatographic method indicated that histamine and cadaverine levels in white cheese sample were below the detection limit of the biosensor method. Therefore recovery experiments in this cheese sample were carried out to demonstrate the practical use of the presented biosensors. DAO/ITONP/PB/SPCE exhibited the highest sensitivity to histamine and recovery experiments were performed using histamine. The recovery experiments were performed by spiking known amounts of histamine to the electrochemical cell. The amount of histamine in spiked sample was determined by standard addition method. The same experiment was performed for cadaverine to investigate the applicability of MAO/ITONP/PB/SPCE since this biosensor exhibited the highest sensitivity to cadaverine. Recoveries of histamine and cadaverine from spiked white cheese sample determined by the DAO/ITONP/PB/SPCE and MAO/ITONP/PB/SPCE biosensors are presented in Table 2. The recoveries varied in the range from 101 to 103% for histamine and 103 to 105% for cadaverine, indicating that the accuracy of the proposed biosensor method is quite good.

The results of DAO/ITONP/PB/SPCE and MAO/ITONP/PB/SPCE biosensors and HPLC method for histamine and cadaverine content in aged kashar cheese sample is presented in Table 3. As can be seen, the results of DAO/ITONP/PB/SPCE biosensor and HPLC are in good agreement. The accuracy of the biosensor method was also checked by *t*-test. The $t_{experimental}$ value is 2.70 for DAO/ITONP/PB/SPCE at 95% confidence level, for which t_{critic} is 2.78. The *t* test indicates that there is no difference between the results of two methods at a confidence level of 95%. On the other hand, cadaverine level detected in aged kashar cheese was below the detection limit of the MAO/ITONP/PB/SPCE biosensor.

Histamine and cadaverine content of İzmir tulum cheese sample was also investigated by the biosensor method and compared with conventional HPLC method (Table 3). Comparable results between both methods at 95% confidence level were obtained. The accuracy of the method was investigated by *t*-test. The $t_{experimental}$ value for DAO/ITONP/PB/SPCE and MAO/ITONP/PB/SPCE were found as 2.61 and 2.46, respectively, for which t_{critic} is 2.78. It can be concluded that no significant differences

Table 2 Recoveries of histamine and cadaverine from spiked white cheese sample determined by the DAO/ITONP/PB/SPCE and MAO/ITONP/PB/SPCE biosensors

Histamine (mg L^{-1})			Cadaverine (mg L^{-1})		
DAO/ITONP/PB/SPCE			MAO/ITONP/PB/SPCE		
Added	Found*	Recovery, %*	Added	Found*	Recovery, %*
1.10	1.13	103.0 ± 9.8	0.70	0.74	104.9 ± 9.5
1.46	1.47	101.1 ± 7.4	1.04	1.09	104.5 ± 6.3
1.82	1.87	102.8 ± 5.9	1.39	1.43	103.2 ± 4.7

*Results represent the mean of three measurements ($N = 3$)

Table 3 Results of histamine and cadaverine contents in cheese samples obtained from presented biosensors and HPLC

Sample	Histamine (mg L^{-1})		Cadaverine (mg L^{-1})	
	DAO/ITO/PB/SPCE	HPLC	MAO/ITO/PB/SPCE	HPLC
Aged kashar cheese	5.82 ± 0.17	5.71 ± 0.06	ND	0.50 ± 0.04
İzmir tulum cheese	1.73 ± 0.05	1.69 ± 0.04	19.17 ± 0.49	18.88 ± 0.14

Results represent the mean of three measurements ($N = 3$) *ND*: not detected

were observed between the results obtained with the presented biosensors and reference HPLC method. Satisfactory correlation between the results of the HPLC and biosensor methods indicated that DAO/ITONP/PB/SPCE and MAO/ITONP/PB/SPCE biosensors are promising approaches for biogenic amine determination in cheese samples.

Conclusion

In this study, a new sensing platform for the determination of biogenic amines is reported based on screen-printed carbon electrodes modified with PB and ITO nanoparticles. The composite use of the PB and ITO nanoparticles improved the performance of the presented biosensors and the biosensors exhibited good repeatability and reproducibility, wide linear range and low detection limit towards histamine, cadaverine and putrescine determination. The successful application in the determination of histamine and cadaverine in cheese samples demonstrated that the presented biosensors possess a great potential for simple and rapid analysis of these biogenic amines in food samples.

Funding information This work was financially supported by The Scientific and Technical Research Council of Turkey (TUBITAK Project No.: 116Z159).

Compliance with ethical standards

Conflict of interest The authors declare that they have no conflict of interest.

References

1. Calvo-Pérez A, Domínguez-Renedo O, Alonso-Lomillo MA, Arcos-Martínez MJ. Disposable amperometric biosensor for the determination of tyramine using plasma amino oxidase. Microchim Acta. 2013;180(3–4):253–9.
2. Shalaby AR. Significance of biogenic amines to food safety and human health. Food Res Int. 1996;29(7):675–90.
3. Henao-Escobar W, Domínguez-Renedo O, Alonso-Lomillo MA, Arcos-Martínez MJ. Simultaneous determination of cadaverine and putrescine using a disposable monoamine oxidase based biosensor. Talanta. 2013;117:405–11.
4. Carelli D, Centonze D, Palermo C, Quinto M, Rotunno T. An interference free amperometric biosensor for the detection of biogenic amines in food products. Biosens Bioelectron. 2007;23(5):640–7.
5. Romano A, Klebanowski H, La Guerche S, Beneduce L, Spano G, Murat M-L, et al. Determination of biogenic amines in wine by thin-layer chromatography/densitometry. Food Chem. 2012;135(3):1392–6.
6. Lapa-Guimaraes J, Pickova J. New solvent systems for thin-layer chromatographic determination of nine biogenic amines in fish and squid. J Chromatogr A. 2004;1045(1–2):223–32.
7. Shalaby A. Simple, rapid and valid thin layer chromatographic method for determining biogenic amines in foods. Food Chem. 1999;65(1):117–21.
8. Almeida C, Fernandes J, Cunha S. A novel dispersive liquid–liquid microextraction (DLLME) gas chromatography-mass spectrometry (GC–MS) method for the determination of eighteen biogenic amines in beer. Food Control. 2012;25(1):380–8.
9. Innocente N, Biasutti M, Padovese M, Moret S. Determination of biogenic amines in cheese using HPLC technique and direct derivatization of acid extract. Food Chem. 2007;101(3):1285–9.
10. Önal A. A review: current analytical methods for the determination of biogenic amines in foods. Food Chem. 2007;103(4):1475–86.
11. Önal A, Tekkeli SEK, Önal C. A review of the liquid chromatographic methods for the determination of biogenic amines in foods. Food Chem. 2013;138(1):509–15.
12. Bóka B, Adányi N, Virág D, Sebela M, Kiss A. Spoilage detection with biogenic amine biosensors, comparison of different enzyme electrodes. Electroanalysis. 2012;24(1):181–6.
13. Leonardo S, Campàs M. Electrochemical enzyme sensor arrays for the detection of the biogenic amines histamine, putrescine and cadaverine using magnetic beads as immobilisation supports. Microchim Acta. 2016;183(6):1881–90.
14. Aigner M, Telsnig D, Kalcher K, Teubl C, Macheroux P, Wallner S, et al. Amperometric biosensor for total monoamines using a glassy carbon paste electrode modified with human monoamine oxidase B and manganese dioxide particles. Microchim Acta. 2015;182(5–6):925–31.
15. Boffi A, Favero G, Federico R, Macone A, Antiochia R, Tortolini C, et al. Amine oxidase-based biosensors for spermine and spermidine determination. Anal Bioanal Chem. 2015;407(4):1131–7.
16. Dalkıran B, Erden PE, Kaçar C, Kılıç E. Disposable Amperometric biosensor based on poly-L-lysine and Fe3O4 NPs-chitosan composite for the detection of Tyramine in cheese. Electroanalysis. 2019;31(7):1324–33.
17. Shi X, Gu W, Li B, Chen N, Zhao K, Xian Y. Enzymatic biosensors based on the use of metal oxide nanoparticles. Microchim Acta. 2014;181(1–2):1–22.
18. Liu B, Liu J. DNA adsorption by indium tin oxide nanoparticles. Langmuir. 2014;31(1):371–7.
19. Sivasakthi P, Bapu GR, Chandrasekaran M. Pulse electrodeposited nickel-indium tin oxide nanocomposite as an electrocatalyst for non-enzymatic glucose sensing. Mater Sci Eng C. 2016;58:782–9.
20. Aydın EB, Sezgintürk MK. Indium tin oxide (ITO): a promising material in biosensing technology. TrAC Trends in Anal Chem. 2017;97:309–15.
21. Wang J, Wang L, Di J, Tu Y. Disposable biosensor based on immobilization of glucose oxidase at gold nanoparticles electrodeposited on indium tin oxide electrode. Sens Actuators B: Chemical. 2008;135(1):283–8.
22. El-Said WA, Choi J-W. Electrochemical biosensor consisted of conducting polymer layer on gold nanodots patterned indium tin oxide electrode for rapid and simultaneous determination of purine bases. Electrochim Acta. 2014;123:51–7.
23. Liang F, Jia M, Hu J. Pt-implanted indium tin oxide electrodes and their amperometric sensor applications for nitrite and hydrogen peroxide. Electrochim Acta. 2012;75:414–9.
24. Rigoni F, Drera G, Pagliara S, Goldoni A, Sangaletti L. High sensitivity, moisture selective, ammonia gas sensors based on single-walled carbon nanotubes functionalized with indium tin oxide nanoparticles. Carbon. 2014;80:356–63.
25. Bobrowski T, Arribas EG, Ludwig R, Toscano MD, Shleev S, Schuhmann W. Rechargeable, flexible and mediator-free biosupercapacitor based on transparent ITO nanoparticle modified electrodes acting in μM glucose containing buffers. Biosens Bioelectron. 2018;101:84–9.
26. Chen X, Wu G, Cai Z, Oyama M, Chen X. Advances in enzyme-free electrochemical sensors for hydrogen peroxide, glucose, and uric acid. Microchim Acta. 2014;181(7–8):689–705.

27. Erden PE, Kılıç E. A review of enzymatic uric acid biosensors based on amperometric detection. Talanta. 2013;107:312–23.
28. Benedet J, Lu D, Cizek K, La Belle J, Wang J. Amperometric sensing of hydrogen peroxide vapor for security screening. Anal Bioanal Chem. 2009;395(2):371–6.
29. Özdemir DS, Kaçar C, Dalkıran B, Küçükkolbaşı S, Erden PE, Kılıç E. Effect of hexaammineruthenium chloride and/or horseradish peroxidase on the performance of hydrogen peroxide (bio) sensors: a comparative study. J Mater Sci. 2019;54(7):5381–98.
30. Karyakin AA, Karyakina EE. Prussian blue-basedartificial peroxidase'as a transducer for hydrogen peroxide detection. Application to biosensors. Sens Actuators B: Chemical. 1999;57(1–3):268–73.
31. Karyakin AA, Karyakina EE, Gorton L. Amperometric biosensor for glutamate using prussian blue-based "artificial peroxidase" as a transducer for hydrogen peroxide. Anal Chem. 2000;72(7):1720–3.
32. Ricci F, Amine A, Palleschi G, Moscone D. Prussian blue based screen printed biosensors with improved characteristics of long-term lifetime and pH stability. Biosens Bioelectron. 2003;18(2–3):165–74.
33. Garjonyte R, Yigzaw Y, Meskys R, Malinauskas A, Gorton L. Prussian blue-and lactate oxidase-based amperometric biosensor for lactic acid. Sens Actuators B: Chemical. 2001;79(1):33–8.
34. Li M, Li Y-T, Li D-W, Long Y-T. Recent developments and applications of screen-printed electrodes in environmental assays—a review. Anal Chim Acta. 2012;734:31–44.
35. Taleat Z, Khoshroo A, Mazloum-Ardakani M. Screen-printed electrodes for biosensing: a review (2008–2013). Microchim Acta. 2014;181(9–10):865–91.
36. Sekar NC, Shaegh SAM, Ng SH, Ge L, Tan SN. A paper-based amperometric glucose biosensor developed with Prussian blue-modified screen-printed electrodes. Sens Actuators B: Chemical. 2014;204:414–20.
37. Liu X, Li X, Gao X, Ge L, Sun X, Li F. A universal paper-based electrochemical sensor for zero-background assay of diverse biomarkers. ACS Appl Mater Interfaces. 2019;11(17):15381–8.
38. Teng Y, Zuo S, Lan M. Direct electron transfer of horseradish peroxidase on porous structure of screen-printed electrode. Biosens Bioelectron. 2009;24(5):1353–7.
39. Compagnone D, Isoldi G, Moscone D, Palleschi G. Amperometric detection of biogenic amines in cheese using immobilised diamine oxidase. Anal Lett. 2001;34(6):841–54.
40. Zotou A, Loukou Z, Soufleros E, Stratis I. Determination of biogenic amines in wines and beers by high performance liquid chromatography with pre-column dansylation and ultraviolet detection. Chromatographia. 2003;57:429–39.
41. Martín M, González Orive A, Lorenzo-Luis P, Hernández Creus A, González-Mora JL, Salazar P. Quinone-rich poly (dopamine) magnetic nanoparticles for biosensor applications. ChemPhysChem. 2014;15(17):3742–52.
42. Tsai Y-C, Chiu C-C. Amperometric biosensors based on multiwalled carbon nanotube-Nafion-tyrosinase nanobiocomposites for the determination of phenolic compounds. Sens Actuators B: Chemical. 2007;125(1):10–6.
43. Pandey PC, Pandey AK, Chauhan DS. Nanocomposite of Prussian blue based sensor for L-cysteine: synergetic effect of nanostructured gold and palladium on electrocatalysis. Electrochim Acta. 2012;74:23–31.
44. Wang B, Ji X, Zhao H, Wang N, Li X, Ni R, et al. An amperometric β-glucan biosensor based on the immobilization of bi-enzyme on Prussian blue–chitosan and gold nanoparticles–chitosan nanocomposite films. Biosens Bioelectron. 2014;55:113–9.
45. Luo X, Killard AJ, Smyth MR. Reagentless glucose biosensor based on the direct electrochemistry of glucose oxidase on carbon nanotube-modified electrodes. Electroanalysis: An International Journal Devoted to Fundamental and Practical Aspects of Electroanalysis. 2006;18(11):1131–4.
46. Ricci F, Palleschi G. Sensor and biosensor preparation, optimisation and applications of Prussian blue modified electrodes. Biosens Bioelectron. 2005;21(3):389–407.
47. Cinti S, Arduini F, Moscone D, Palleschi G, Killard A. Development of a hydrogen peroxide sensor based on screen-printed electrodes modified with inkjet-printed Prussian blue nanoparticles. Sensors. 2014;14(8):14222–34.
48. Keow CM, Bakar FA, Salleh AB, Heng LY, Wagiran R, Bean LS. An amperometric biosensor for the rapid assessment of histamine level in tiger prawn (Penaeus monodon) spoilage. Food Chem. 2007;105(4):1636–41.
49. Alonso-Lomillo MA, Domínguez-Renedo O, Matos P, Arcos-Martínez MJ. Disposable biosensors for determination of biogenic amines. Anal Chim Acta. 2010;665(1):26–31.
50. Pérez S, Bartrolí J, Fàbregas E. Amperometric biosensor for the determination of histamine in fish samples. Food Chem. 2013;141(4):4066–72.
51. Gumpu MB, Nesakumar N, Sethuraman S, Krishnan UM, Rayappan JBB. Development of electrochemical biosensor with ceria–PANI core–shell nano-interface for the detection of histamine. Sens Actuators B: Chemical. 2014;199:330–8.
52. Vanegas D, Patiño L, Mendez C, Oliveira D, Torres A, Gomes C, et al. Laser scribed graphene biosensor for detection of biogenic amines in food samples using locally sourced materials. Biosensors. 2018;8(2):42.
53. Torre R, Costa-Rama E, Lopes P, Nouws HP, Delerue-Matos C. Amperometric enzyme sensor for the rapid determination of histamine. Anal Methods. 2019;11(9):1264–9.
54. Piermarini S, Volpe G, Federico R, Moscone D, Palleschi G. Detection of biogenic amines in human saliva using a screen-printed biosensor. Anal Lett. 2010;43(7–8):1310–6.
55. Di Fusco M, Federico R, Boffi A, Macone A, Favero G, Mazzei F. Characterization and application of a diamine oxidase from Lathyrus sativus as component of an electrochemical biosensor for the determination of biogenic amines in wine and beer. Anal Bioanal Chem. 2011;401(2):707–16.
56. Shanmugam S, Thandavan K, Gandhi S, Sethuraman S, Rayappan JBB, Krishnan UM. Development and evaluation of a highly sensitive rapid response enzymatic nanointerfaced biosensor for detection of putrescine. Analyst. 2011;136(24):5234–40.
57. Gumpu MB, Nesakumar N, Sethuraman S, Krishnan UM, Rayappan JBB. Determination of putrescine in tiger prawn using an amperometric biosensor based on immobilization of diamine oxidase onto ceria nanospheres. Food Bioprocess Technol. 2016;9(4):717–24.
58. Henao-Escobar W, Domínguez-Renedo O, Alonso-Lomillo MA, Arcos-Martínez MJ. A screen-printed disposable biosensor for selective determination of putrescine. Microchim Acta. 2013;180(7–8):687–93.
59. Niculescu M, Nistor C, Frébort I, Peč P, Mattiasson B, Csöregi E. Redox hydrogel-based amperometric bienzyme electrodes for fish freshness monitoring. Anal Chem. 2000;72(7):1591–7.
60. Al Layla AM, Türkarslan Ö, Kurbanoglu S, Sulaiman ST, Al-Flayeh K, Toppare L. A new amperometric biosensor for diamine: use of a conducting polymer layer. J Macromol Sci, Part A. 2013;50(9):914–22.
61. Ov P, Ferreira IM, Mendes E, Oliveira BM, Ferreira M. Effect of temperature on evolution of free amino acid and biogenic amine contents during storage of Azeitão cheese. Food Chem. 2001;75(3):287–91.